Mechanical and natural ventilation systems in a greenhouse designed using computational fluid dynamics

Jorge Flores-Velazquez[1*], Juan I. Montero[2], Esteban J. Baeza[3], Juan C. Lopez[4]

(1. *Mexican Institute of Water Technology. Paseo Cuauhnáhuac 8532, Col. Progreso, C.P. 62550, Jiutepec, Mor. Mexico*;
2. *Institut de Recerca i Tecnologia Agroalimentàries, 08348, Cabrils* (*Barcelona*)*, Spain*;
3. *IFAPA Centro La Mojonera (Junta de Andalucía), Camino San Nicolás 1, 04745 La Mojonera, Almería, Spain*;
4. *Fundación Cajamar. Estación Experimental "Las Palmerillas" Autovía del Mediterráneo Km 416,7 04710, El Ejido, Almería, Spain*)

Abstract: The aim of this study was to analyse air exchange and temperature distribution in a greenhouse with combined mechanical and natural ventilation and to design more efficient mechanical ventilation systems. For this purpose, a computational fluid dynamics (CFD) model of the greenhouse was used. Three configurations were considered: Configuration 1 (mechanical ventilation and closed roof ventilators), Configurations 2 and 3 (mechanical ventilation and roof ventilators open 30% and 100%, respectively). After validation, the CFD model was used to improve the design of the greenhouse mechanical ventilation system in each of the three configurations analyzed. Four greenhouse lengths, 28 m, 50 m, 75 m and 100 m, were used in the simulations. Compared to fan ventilation only, roof ventilation improved the climate of fan-ventilated greenhouses in terms of the air exchange rate (22%) and climate uniformity because the internal air was mixed better than with mechanical ventilation only. As the greenhouse length increased, more advantages were achieved with natural ventilation compared to mechanical ventilation. For most configurations, there was a strong linear correlation between temperature gradient and greenhouse length. The greenhouse whose regression line had the steepest slope was the one with closed roof ventilators. Increasing the fan capacity produced a general reduction in temperature, but the effect was less intense for the greenhouses with open roof ventilators. Compared to box inlet ventilators, an enlarged continuous inlet in the wall opposite the fans increased overall system performance because it eliminated backflow recirculation zones, which are prone to produce high temperatures.

Keywords: greenhouse cooling, fan ventilation, roof ventilators, combined ventilation
DOI: 10.3965/j.ijabe.20140701.001

Citation: Flores-Velazquez J, Montero J I, Baeza E J, Lopez J C. Mechanical and natural ventilation systems in a greenhouse designed using computational fluid dynamics. Int J Agric & Biol Eng, 2014; 7(1): 1－16.

1 Introduction

Efficient greenhouse ventilation is essential under most climate conditions, including northern regions with cold and humid winters and semi-arid regions with hot summers. In the first case, ventilation helps reduce excessive humidity to prevent crop mineral depletion and fungal diseases[1]. In semi-arid regions, it is very important to control the inside temperature and relative humidity to maintain plant photosynthetic and transpiration rates[1]. Natural ventilation is one of the cheapest ways to regulate the microclimate of internal greenhouse. However, the need to protect crops from pest attacks by using insect-proof screens leads to a sharp reduction in air exchange rates in greenhouses with natural ventilation. Insect-proof screens have been reported to reduce ventilation efficiency by about 50%[2,3].

Received date: 2013-06-26 **Accepted date**: 2014-01-09
Biographies: Juan I. Montero, PhD, Chef of Biosystem Department, expert in high technology in the greenhouse system. **Esteban J. Baeza**, Researcher, dedicated to innovation in greenhouse system. **Juan C. Lopez**, PhD, expert in climate control in greenhouses.
***Corresponding author: Jorge Flores-Velazquez**, PhD, research concentrated in irrigation engineering and computational fluid dynamics analysis in greenhouses environments; Tel: +52 (777) 329 3658. Mexican Institute of Water Technology, Paseo Cuauhnáhuac 8532, Col. Progreso, C.P. 62550, Jiutepec, Mor. Mexico; Tel: +52 (777) 329 3658; Email: jorge_flores@tlaloc.imta.mx.

Moreover, natural ventilation is highly dependent on outside environmental conditions, thus making it difficult to control. Mechanical ventilation could therefore be a good way to improve climate control in screened greenhouses.

Around the world, greenhouse mechanical ventilation has been used less than natural ventilation possibly due to differences in energy and maintenance demands from the the two systems. There is scarce literature of research on this topic to the authors' knowledge. The American Society of Agricultural and Biological Engineers[4] provides guidelines for the procedure of designing mechanical ventilation systems. These guidelines are useful, but many of them are empirical rules that are not always valid for conditions other than those for which they were established. Willits et al.[5] discussed the limitations of the ASABE guidelines, such as the difficulty of using approximate values for the transpiration coefficient in the design and calculation of the ventilation system.

There are few studies exclusively on the topic of mechanical ventilation[2,6]. In many cases, exhaust fans are considered to be part of evaporative cooling systems, such as the fan and pad cooling system. For instance, Montero et al.[7] compared three methods of evaporative cooling and their effects on air and leaf temperature. The fan and pad system reduced leaf temperature near the pad by 3ºC compared to the outside air temperature, but it is effectively decreased as the distance from the cooling pad increased. At the fan end of a 30-m-long greenhouse, leaf and air temperatures were higher than the outside air temperature.

The development of temperature and humidity gradients along the direction of the airflow in fan-ventilated greenhouses has been identified as a major problem in this type of cooling system. Willits et al.[5] pointed out that there could be a lack of homogeneity in the internal climate when mechanical ventilation is used. Under very arid conditions, temperature differences of nearly 15ºC were reported in a 38-m-long fan and pad cooled greenhouse[8]. Arbel et al.[9] compared two mechanically ventilated greenhouse compartments, one operating with a fan and pad system and the other with a fog system. They found more uniform temperature and relative humidity conditions in the compartment with the fog system compared to a linear increase of air temperature with distance in the greenhouse with fan and pad cooling. Kittas et al.[10,11] found that the vertical gradients of air temperature and humidity were more homogeneous with mechanical ventilation than those with natural ventilation. The same authors suggested the use of shading for the second half of a long greenhouse to reduce temperature gradients.

Other authors mentioned that climate homogeneity can be improved if the roof ventilators are left partially open, so that mechanical ventilation is combined with natural ventilation[12,13]. Studies on the combination of the two air exchange methods are rather limited.

Most of the information available on mechanical ventilation comes from studies mainly descriptive. For example, Al-Helal[8] compared the effects of two ventilation rates on greenhouse climate, but the study was merely descriptive. More analysis is needed to fully understand the effects of relevant parameters on greenhouse climate, such as the fan air exchange rate, greenhouse length and the combination of roof ventilation and mechanical ventilation.

More recently, numerical analysis such as computational fluid dynamics (CFD) has been used to obtain more information on the spatial distribution of climate inside the greenhouse[14]. The CFD is a valuable tool for the analysis of ventilation systems because it provides a detailed analysis of the ventilation process and, therefore, of relevant climatic variables[15,16]. Questions on the management of ventilation to produce sufficient air movement and quantify the levels of heat and mass transfer between the crop and the surrounding air can be answered through the application of CFD[1,15,17-20]. The CFD can be used to improve the design and management of mechanical ventilation systems.

The aim of this study was to analyse air exchange and temperature distribution in a greenhouse with combined mechanical and natural ventilation systems and to design more efficient mechanical ventilation systems.

2 Materials and methods

2.1 Experimental greenhouse

The experiment was carried out in an East-West three-span greenhouse located in Almería, Southern Spain (latitude 36º48′, longitude 2º43′ and altitude 151 m), near the Mediterranean coast. The geometrical characteristics of the greenhouse were given as follows: width, 22.5 m; length, 28 m (639 m^2 soil-covered area); eave height, 3 m; and ridge height, 4.7 m; total volume, 2 614 m^3. The mechanical ventilation system consisted of one exhaust fan (1.4 × 1.4 m EX50"-1.5, EXAFAN, Spain) per greenhouse span. The main air inlets consisted of rectangular boxes (2 × 1.4 × 1.15 m) located on the front wall of each span, opposite to the exhaust fans (Figure 1). The greenhouse had three roof ventilators along the main axis of the greenhouse with a maximum opening of 1 m (Figure 1). The roof ventilators were partially open (30%), totally open (100%) and closed (0%) to provide the three different ventilation configurations studied. All the openings were covered with an insect-proof screen (22.5 by 11 threads per centimeter, 25% porosity and 0.3-mm thread thickness). The greenhouse was covered with 0.2-mm-thick polyethylene film.

The experiment was performed in an empty greenhouse (no crops), which can be assumed to be the scenario of a recently transplanted crop, since this is the most unfavourable case in terms of maximum internal temperatures. Measurements were taken for the greenhouse ventilation rate and the internal air temperature profiles in order to compile data to validate the CFD simulations. These measurements were carried out from 24 April to 8 June, 2007.

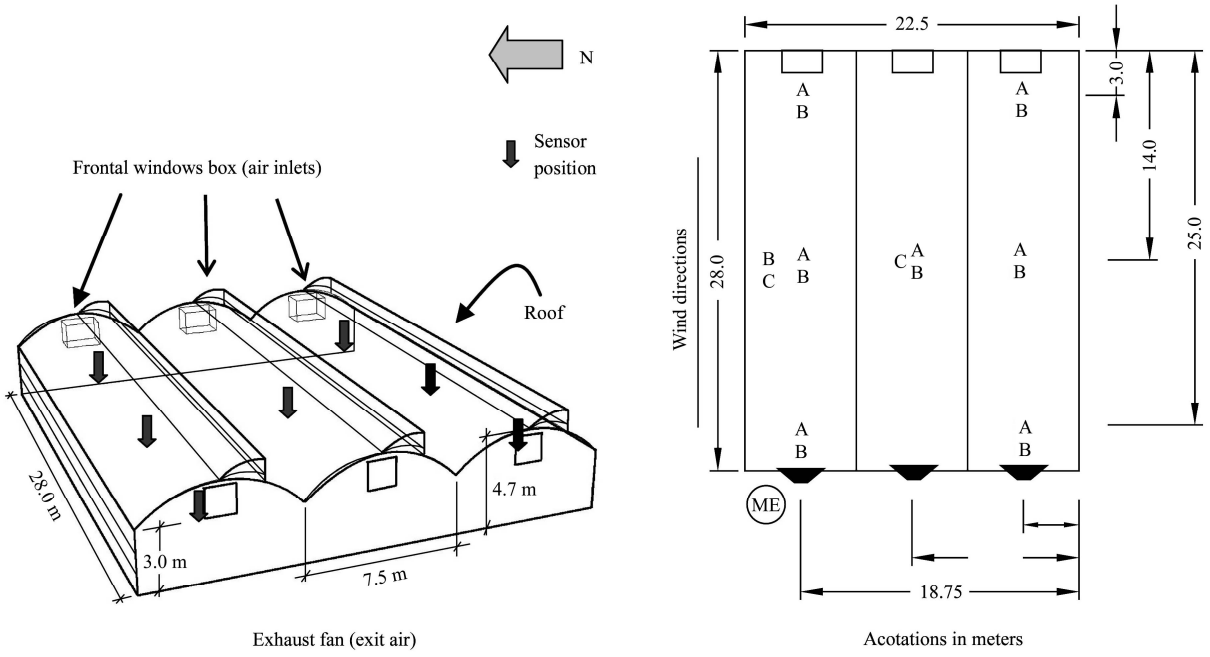

Figure 1 Layout of the experimental greenhouse design and temperature sensor distribution.
A - Dry bulb temperature, B - Soil heat flux plate, C - Soil temperature. Lengths are given in meter.

2.1.1 Tracer gas measurements

The greenhouse air exchange rate was determined using the decay rate method with N_2O as the dynamic tracer gas[21]. A Siemens ULTRAMAT 5M sensor (Germany) was used to measure the decay rate concentration. A mathematical development of this method can be found in the study by Boulard and Draoui[22]. Roy et al.[23] provided a detailed description of the procedure for the decay rate measurement. The variation in the concentration of the tracer gas over time follows logarithmic behaviour, as described in Equation (1).

$$c(t) = c_o \times e^{-V_t} \quad (1)$$

where, c is the tracer gas concentration (ppm) at time t (s); c_o is the initial tracer gas concentration (ppm) and V_t is the air exchange rate (h^{-1}), identified as the number of

greenhouse air exchanges per hour, which was calculated using Equation (2).

$$-V_t = \ln \frac{c(t)}{c_o} \quad (2)$$

2.1.2 Climate variables

Air temperature was measured at seven positions inside the greenhouse at a height of 1 m. Soil temperature was measured at eight positions in the greenhouse and heat flux transfer was measured at two positions. A schematic of the distribution of the sensors is shown in Figure 1. Specific features of the sensors were: A. Dry bulb temperature Pt-100, PRIVA Maximizer, the Netherlands; B. Soil Heat Flux Plate, HFT3-L, REBS, Campbell Sci, USA; C. Soil temperature, 107-L Temperature Probe (negative 35°C to 50°C), Campbell Sci, USA. Outside air climate variables were recorded at a nearby, on top the greenhouse, meteorological station with a radiation sensor (Global solar Radiation Model CM11 Thies Clima, Germany; Wind Vane Anemometer, Class Standard, Thies Clima, Germany; Dry and wet bulb temperature, Pt-100, PRIVA Maximizer, the Netherlands). Experimental data were stored in a CR21 logger (Campbell, USA).

For each combination of roof ventilators, air temperature data were gathered at seven different positions on a horizontal plane at a height of 1 m for one hour. The scan interval of the reading from the sensors was one data each 5 min average of every 30 s. All data selected for analysis were obtained from a daily interval of 30 min at solar noon, when the most adverse weather conditions are expected. Environmental temperature and its analysis data were the averages of 30 min between 11:20 and 11:50 solar height at 1 m and from 12:00 to 12:30 with the solar height at 2 m.

2.2 Numerical model

Navier-Stokes (N-S) equations provide the mathematical description of air movement inside the greenhouse. Air is assumed to be a viscous incompressible fluid. A numerical solution of the N-S equations produces the velocity field $u(x,t)=(u_1(x,t), u_2(x,t), u_3(x,t))$ of a particle at each location $x=(x_1, x_2, x_3, t)$ in the three-dimensional domain at time t, as well as the pressure $p=p(x,t)$ of the fluid[24].

The equation describing the transport phenomena for a steady flow in free convection can be written as follows[25].

$$\frac{\partial(\rho\phi)}{\partial t} + \nabla \cdot (\partial \overline{u}\phi) = \nabla \cdot (\Gamma \nabla \phi) + S\phi \quad (3)$$

Equation (3) shows four terms: instability, convection, diffusion and a source term where the variable ϕ is the dependent variable that describes the flux characteristics at a specific point and time; ρ is fluid density, u represents the air velocity vector, which, in a 3-D space, would be $\phi = \phi(x, y, z, t)$.

2.2.1 Porous jump condition

The insect-proof screen was modelled as a function of permeability and porosity[26]. The flux movement through a porous media can be modelled using the Forchheimer Equation (4) for highly porous materials.

$$\frac{\partial p}{\partial x} = \frac{\mu}{K}u + \rho\frac{C_F}{\sqrt{K}}u|u| \quad (4)$$

where, ∂p is the drop in pressure through a porous media, Pa; ∂x is the thickness of the porous media, m; μ is the dynamic viscosity of the fluid, kg/(m·s); K is media permeability, m^2; C_F is the inertial factor or non-linear momentum loss coefficient; ρ is the air density, kg/m^3; and u is the air velocity, m/s.

Several screen coefficients for K and C_F can be found in the literature[26-31], but, according to a more recent study by Teitel[32], using these published values may lead to erroneous calculations. Teitel[32] suggested using the experimental measurement of pressure drop in air as a function of upstream air velocity. A wind tunnel is required to do the measurements for this method. Since a wind tunnel was not available for this study, the decision was made to apply Teitel's method to the experimental data obtained by Kamaruddin[29] for a screen that had a porosity of 25%, 20 threads per cm and 0.372 mm thread thickness. For this screen[29] a quadratic regression given by Equation (5) was obtained:

$$\partial p = 2.324u + 2.536u^2 \quad (5)$$

By comparing this experimental regression with Equation (4) it was possible to obtain K and C_F: $\frac{\mu}{K}\rho\,\partial x = 2.324$. For μ = 1.79E-5 kg/(m·s), ∂x = 0.372E-3 m and ρ = 1.225 kg/m^3, we obtained K = 2.46472E-9 m^2.

In the same way $\rho \frac{C_F}{\sqrt{K}} \partial x = 2.536$. For ρ = 1.225 kg/m^3, K = 2.46472E-9 m^2, and ∂x = 0.372E-3 m we obtained C_F = 0.321178618. Such K and C_F values were used in the CFD simulations.

2.2.2 Computational model and boundary conditions

GAMBIT and FLUENT 6.2 CFD codes are commercially available[33]. User guide 12.0 (Lebanon, NH, USA) was used to build a mathematical representation of a 3-D computational model. The domain was 88 m in length, 82.5 m in width and 30 m in height. The mesh had a total of 610 572 cells. A numerical solution of the Reynolds-averaged Navier-Stokes equations[25] was obtained over a discretized flow field based on the finite volume method. The Standard K-ε turbulence model[34] and buoyancy effects were selected to simulate airflow. The model was chosen based on previous research on numerical modelling of greenhouse environment[35-36].

Wind direction was considered to be parallel to the main greenhouse axis. Once the CFD model was developed, two sets of simulations were run. The first set was to validate the CFD model by comparing the experimental and modelled air exchange rates and air temperatures. For this comparison, the measured outside air temperature, wind velocity and heat flux from the greenhouse soil to the air were used as inputs for the CFD simulations. The input parameters are shown in Table 1.

Table 1 Boundary conditions for computational fluid dynamics (CFD) simulations. Boundary conditions were different for model validation than for design studies.

Initial Boundary Conditions	Configuration 1	Configuration 2	Configuration 3
CFD model validation: ventilation rate			
Temperature/K	286	286.5	284.7
Wind Velocity/m·s^{-1}	3.8	2.9	1.7
CFD model validation: temperature			
Temperature/K	297	298.5	295
Wind Velocity/m·s^{-1}	2.5	1.7	3.5
CFD design studies of air velocity and temperature			
Temperature/K	295	295	295
Wind Velocity/m·s^{-1}	2	2	2

The second set of simulations was performed to compare the three greenhouse roof vent configurations and to study the effects of relevant parameters such as the greenhouse length and fan capacity on the internal temperature. Such configurations were: Configuration 1, mechanical ventilation alone (closed roof ventilators); Configuration 2, mechanical ventilation and roof ventilators open 30%; Configuration 3, mechanical ventilation and roof ventilators open 100%. The input parameters for these simulation comparisons are also shown in Table 1.

As mentioned earlier the heat flux from the greenhouse soil to the air is a boundary condition for the CFD model. It was determined by using the energy balance for the soil (Equation (6)).

$$H_{sc} = RI_a - Q_{soil} - R_\alpha \quad (6)$$

where, H_{sc} is the heat transferred from the soil surface to the greenhouse air (W/m^2); RI_a is the fraction of radiation that passes through the film cover (W/m^2) in this case:

$$RIa = RI * \gamma$$

where, RI is the outside solar radiation (W/m^2), the average was 846 W/m^2; γ is the overall greenhouse transmissivity measured as 0.71[37]. Q_{soil} is the soil heat flux to the deep ground, the average experimental value was 159 W/m^2[37]; R_α is the radiation fraction reflected, in this case $R_\alpha = RI_a * \alpha$, α is the albedo (for sandy soil =0.21)[38].

Using these values in Equation (6), the heat transferred to the greenhouse air was 315 W/m^2. Therefore, a constant heat source from the soil surface to the greenhouse air of the same magnitude was simulated to study the system performance under unfavourable hot conditions. The fan curve of the exhaust fans relating airflow and pressure head was implemented in the CFD code to calculate airflow extraction.

3 Results and discussion

The CFD model was first validated against experimental data. For this purpose, CFD simulations were compared with tracer gas measurements of ventilation rate and temperature profiles along the greenhouse length. After validation, a number of

simulations were run for different combinations of greenhouse lengths, roof ventilator openings and fan power to study the temperature gradient along the greenhouse length. Finally, additional simulations were performed to improve the design of the air inlet in the front wall opposite to the fan location.

3.1 Comparison of field experimentation with numerical model simulations

3.1.1 Air exchange rate

Figure 2 shows the relationship between the experimental air exchange rate and wind speed for the three greenhouse configurations studied. In all cases, the poor correlation between both variables can be observed. For closed roof ventilators (Figure 2a), the external wind had no appreciable effect on the air exchange rate, since ventilation was purely caused by the exhaust fans. If the roof ventilators were partially or totally open (Figures 2b and 2c), wind speed had no significant effect on the ventilation rate.

For the three configurations, the average ventilation rates were 20.8, 26.6 and 24.9 air changes per hour, respectively. Assuming that the fans provided the same airflow, regardless of the roof ventilator configuration, most of the air exchange (20.8 air exchanges per hour) was due to mechanical ventilation and little air was exchanged through the roof ventilators.

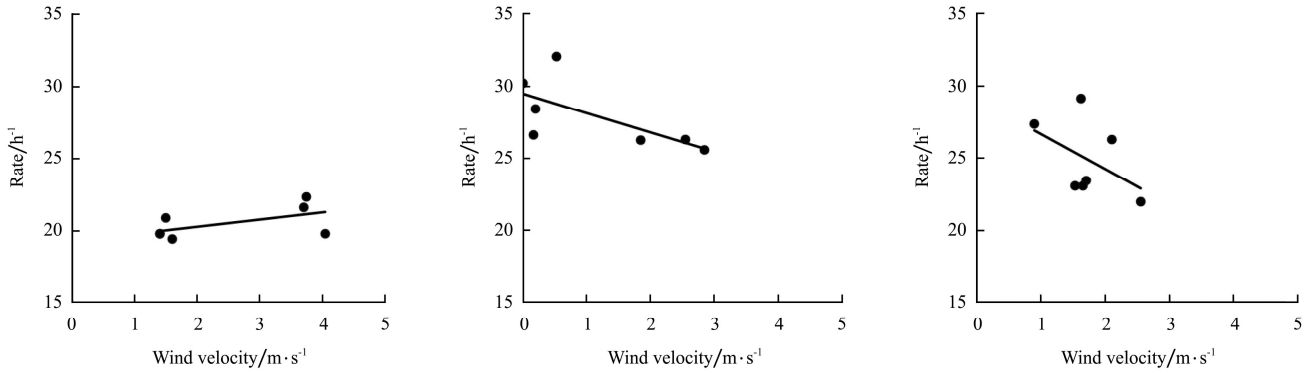

a. Configuration 1 b. Configuration 2 c. Configuration 3

Figure 2 Experimental air exchange rate (per hour) as a function of the wind speed wind velocity

In accordance with Figure 2, Configuration 2 gave slightly higher ventilation rate than Configuration 3; this is an unexpected result since the roof ventilator surface was less for Configuration 2. Besides the air exchange rate was slightly higher at lower wind speeds than that at higher wind speeds (Figures 2b and 2c) which was also unexpected.

Two major reasons can help to explain such apparent discrepancies. On the one hand, the decay rate method has limitations, such as the difficulty of having a perfectly homogeneous gas concentration[22]. It has been reported that the decay rate method has an accuracy of about 30%[39], so the apparent reduction in the ventilation rate with wind speed was within the range of the experimental error in measurement. On the other hand, it is important to note that some experimental measurements were done under low wind speed conditions (less than 4 m/s). Under such conditions, thermally driven ventilation may have played a role in the air exchange process particularly at lower wind speed, and may have caused some air exchange differences between Configurations 2 and 3, since the outside temperatures during measurements were not identical for both configurations.

In order to validate the CFD model, simulations were run with the boundary conditions shown in Table 1. Measured and CFD-calculated air exchange rates for the three configurations considered are presented in Table 2. The agreement was good for the three configurations and the difference between measured and simulated values was within the range of experimental error[22]. For instance, Ould Khaoua et al.[18] reported that CFD simulated ventilation rates were 25% lower on average than experimental values. These differences, which were greater than the ones presented in this study, were attributed mainly to the decay rate method.

Table 2 also shows that air exchange through the roof

ventilators was relatively low compared to the airflow exhausted by the fans. This fact agrees with experimental measurements, as shown in Figure 2. It is noted that not all the roof ventilators performed in the same way; some acted as air inlets and others as air outlets. This topic will be discussed in more detail in the following paragraphs.

Table 2 Air exchange rate (per hour) measured by the tracer gas technique and obtained from the computational fluid dynamics (CFD) model. Negative values mean outlet air while positive values mean inlet air.

	Configuration 1		Configuration 2		Configuration 3	
	Tracer gas	CFD model	Tracer gas	CFD model	Tracer gas	CFD model
Exhaust fan	22.3	25	25.6	21.3	23.4	21.9
Total roof ventilators				1.7		0.9
North				-0.4		-0.8
Centre				-1.3		0.1
South				1.7		0.8
Total greenhouse	22.3	25	25.6	23	23.4	22.8

Table 2 also shows that CFD model gave higher ventilation rate for Configuration 1 (25 per hour) than for Configurations 2 and 3 (23 and 22.8 per hour). As discussed later (Figures 4 and 5), roof ventilation changed the internal pattern of air movement; it had a minor effect on total air exchange rate but had greater effect on air mixing and temperature uniformity.

3.1.2 Temperature profiles

Figure 3 shows the comparison between the experimental and CFD simulated temperatures at a height of 1 m. Each experimental value shown in Figure 3 is the average of the three spans of the experimental greenhouse, measured at 3, 14 and 25 m from the front air inlet wall. Moreover, the represented simulated values are the average of the three temperature profiles along the greenhouse length in each span.

The measured and simulated temperature profiles agreed well in all configurations. The best agreement was for Configuration 3 (Figure 3c, maximum average differences 0.9°C) and the worst for Configuration 2 (Figure 3b, maximum average differences 1.9°C) but in any case the difference between measured and simulated values was less than 2°C. Both the measured and simulated values followed a similar trend. For the three configurations, the lowest temperatures occurred near the air inlet and a temperature gradient was developed along the greenhouse length.

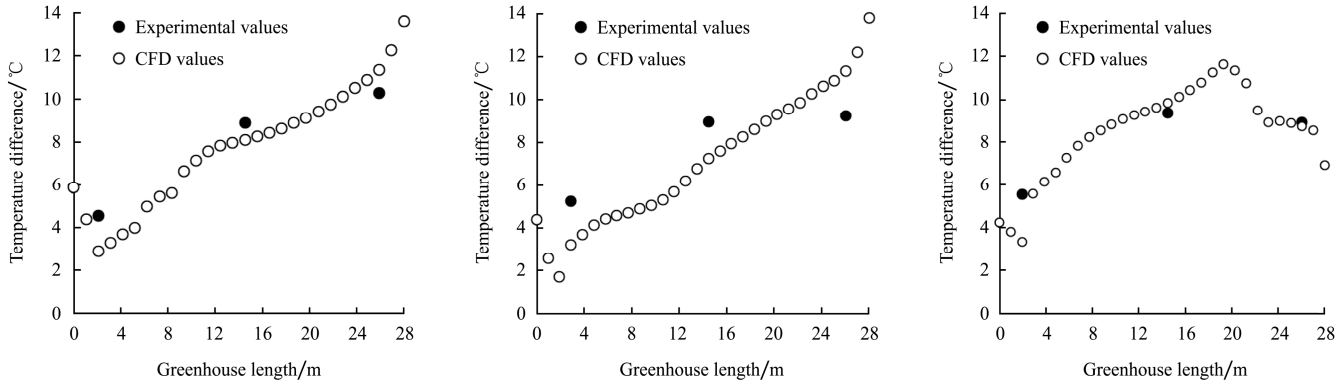

a. Configuration 1 b. Configuration 2 c. Configuration 3

Figure 3 Comparison of experimental and CFD temperature profiles at 1 m height for the three configurations

When the greenhouse roof ventilators were closed, a strong thermal gradient was developed at the air inlet wall (Figure 3a). Roof ventilation contributed to reduce this strong gradient and make the lengthwise temperature profile smoother. The contribution of roof ventilation can be better understood by studying the CFD simulation output (Figures 4 and 5).

Figure 4a shows the velocity field and temperature distribution in the central section of greenhouse Configuration 1. Outside air entered through the front windows; a main air stream travelled close to the greenhouse roof and then went down to the floor area. Two circulation cells were developed: the first one (clockwise) was formed immediately below the screened

entrance box and the second one (counterclockwise) was created near the exit outlet. Normally, circulation cells are areas with higher temperatures (Figure 4b), which may explain the initial and final steps in the temperature profile shown in Figure 3a.

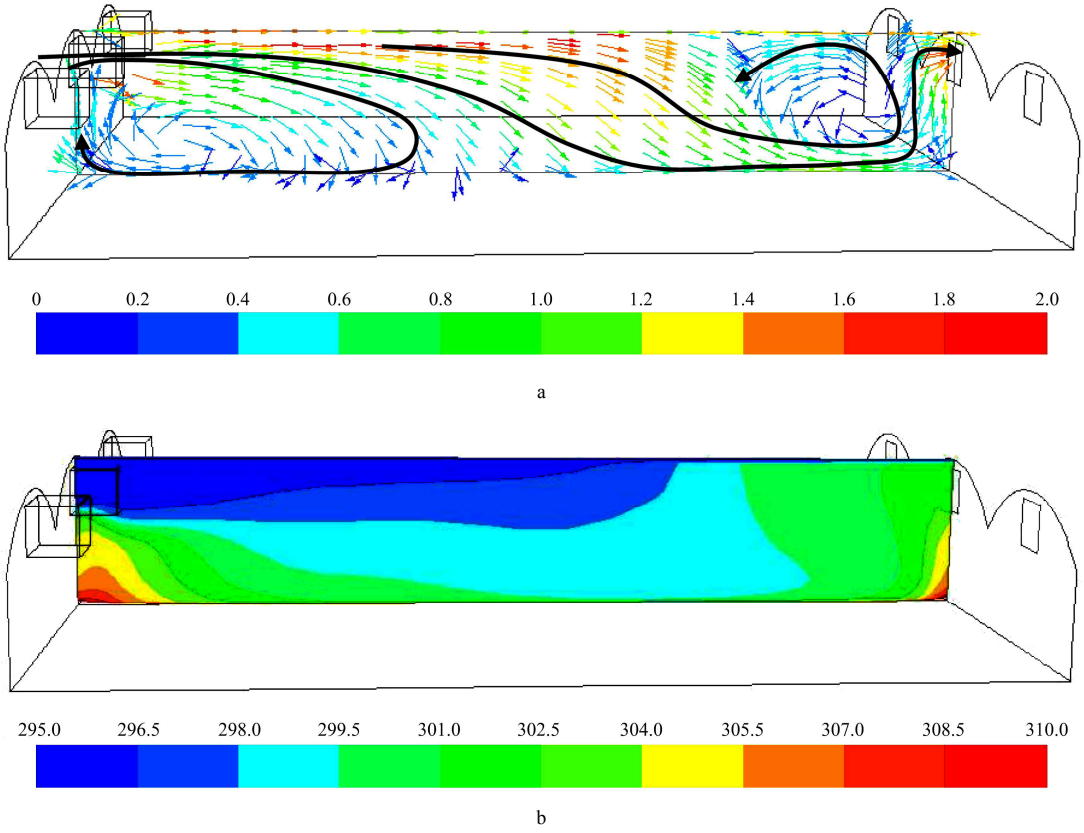

Figure 4 (a) Wind velocity (m s^{-1}) in a vertical plane of the central span for Configuration 1, (b) Air temperature (K) in a vertical plane of the central span for Configuration 1

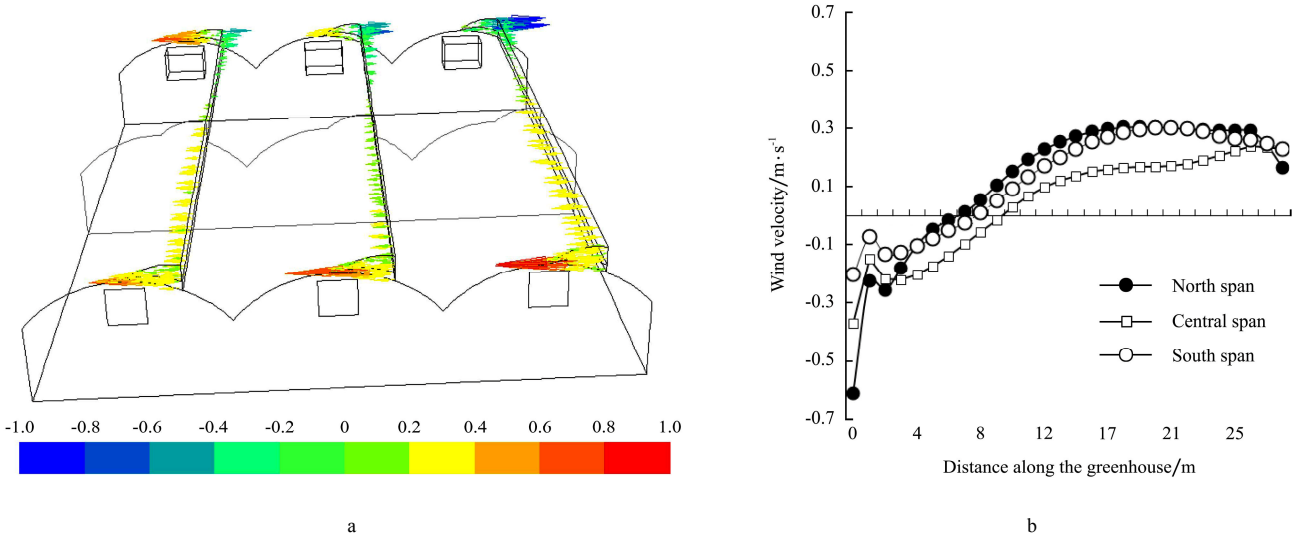

Figure 5 (a) Horizontal component (X axis) of wind velocity (m s^{-1}) in roof ventilators for configuration 3, (b) Wind velocity in roof ventilators

Figure 5 shows the component of air velocity perpendicular to the roof ventilator; part of the internal air exited through the ventilator side closest to the front entrance wall (foreground in Figure 5) and entered through the area closest to the fan (background in Figure 5). A similar behaviour was reported by Boulard et al.[21]

for external winds parallel to the gutter. With roof ventilation, the circulation cells shown in Figure 4a were broken and the step temperature gradients at the entrance and exit (Figure 3a) of the closed-roof greenhouse were reduced. It seems that roof ventilation had a relatively minor effect on total air exchange (Table 2) and overall greenhouse temperature (Figures 3a, 3b and 3c), but had a greater effect on the internal air flow pattern, air mixing and temperature uniformity.

Experimental verification of CFD simulations is a difficult task, given that steady-state CFD simulations produce instantaneous representations of the greenhouse response under a given set of stable external conditions, a situation that rarely takes place in practice. Nevertheless, the similar trend shown in this study in terms of measured and simulated air exchange rates and temperature profiles suggest using this CFD model to improve the design of fan ventilation systems.

3.2 Design of mechanical ventilation systems

3.2.1 Effect of greenhouse length on the temperature regime of mechanically ventilated greenhouses

For the first set of simulations, a relatively low outside air speed of 2 m/s was arbitrarily chosen, since it was intended to study the effect of combined fan ventilation and roof ventilation under unfavourable conditions. Hence, if roof ventilation had a positive effect under low wind conditions, a more positive effect would be expected for higher wind conditions. Four greenhouse lengths were used in the simulations: 28 m (as in the experimental greenhouse), 50 m, 75 m and 100 m. In the first set of simulations and for all greenhouse lengths, the fan airflows were the same as in the 28-m-long experimental greenhouse. For a second set of simulations, the airflow created by the fans was increased to analyse the effect of fan power on temperature distribution.

Configuration 1: Figure 6 shows the temperature distribution at a height of 2 m for the 100-m-long greenhouse. It is clear that temperature increased with greenhouse length; for the first 28 m from the air entrance wall, the increase in temperature compared to the outside air was less than 10 K for all points, whereas for the 100-m-long greenhouse, some hot spots near the central span exit were 320 K (25 K) more than the outside air. The development of a linear temperature gradient in fan-ventilated greenhouses is a well-known fact that limits the recommended distance between air inlets and fan outlets[4]. As discussed in the introduction, this problem can be mitigated by shading the second part of a long greenhouse[11], but this may have direct implications on the crop response due to different light regimes.

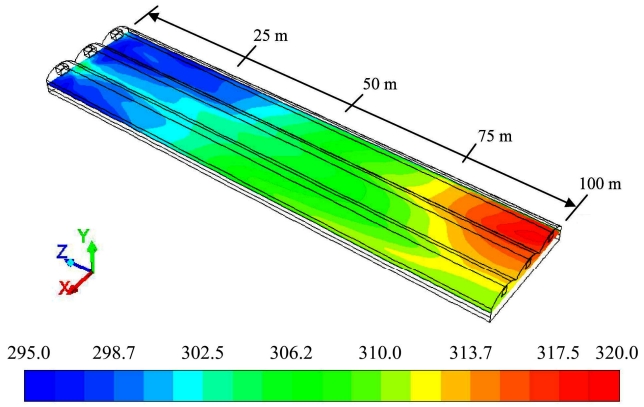

Figure 6 Configuration 1: Map of temperature at 2 m height

Configuration 2: Figure 7 shows that, compared with Configuration 1, roof ventilation produced a general but moderate decrease in temperature, mainly in the area closest to the fan wall. It can also be observed that roof ventilation created a displacement of the warmer areas, given that the hottest spots were near to the south end of the fan wall.

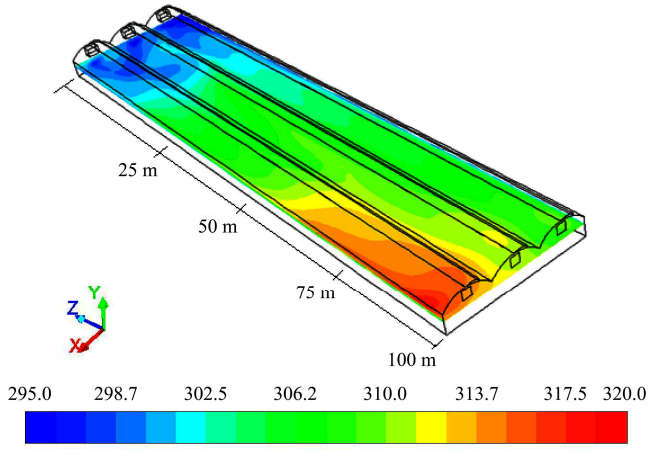

Figure 7 Configuration 2: Map of temperature at 2 m height

Configuration 3: Figure 8 shows a clear reduction in temperature in most of the areas of the 100-m-long greenhouse. It seems that, in spite of the low wind speed used in this study and regardless of the fact that the

external wind was considered parallel to the greenhouse length, natural ventilation played a relevant role in the air exchange process. Table 3 shows the relative importance of mechanical and natural ventilation; for this configuration, some roof ventilators (such as those in the left and right spans) exchanged a greater amount of air than a single fan, whereas air exchange in the central span was relatively low. Table 3 shows the net air exchange rate for each ventilator, i.e. the difference between inlet and outlet air through this specific ventilator. Although the net value was low, the inlet and outlet air volume may have been considerable. Besides increasing the ventilation rate, roof ventilation produced better mixing of the internal air; as a result, the temperature gradient along the greenhouse length observed in Configuration 1 was clearly changed.

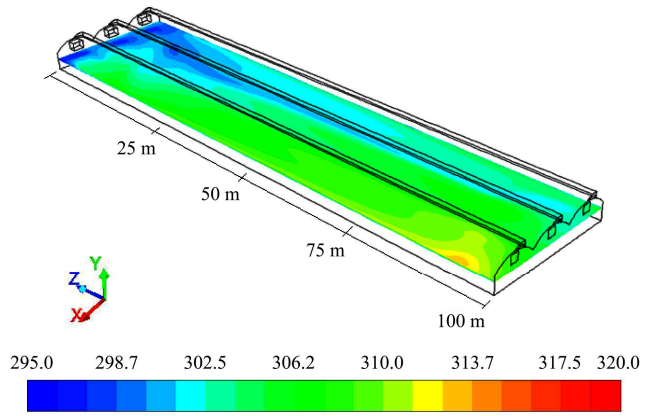

Figure 8 Configuration 3: Map of temperature at 2 m height

Table 3 Air exchange rate (per hour) through the inlet box ventilators and roof ventilators for the three configurations in the 100 m long greenhouse. (Negative values mean outlet air while positive values mean inlet air)

Roof ventilator position	Inlet ventilator	Roof ventilators	Fan ventilators
	Configuration 1		
Left	3.6		-3.6
Central	3.6		-3.6
Right	3.6		-3.7
Total Rate (per hour)	10.9		-10.9
	Configuration 2 Roof windows open 30%		
Left	2	3.2	-3.6
Central	1.9	1.4	-3.6
Right	2	0.2	-3.6
Total Rate (per hour)	5.9	4.9	-10.8
	Configuration 3 Roof windows open 100%		
Left	2	7.1	-3.6
Central	2	2.4	-3.6
Right	2	-4.8	-3.6
Total rate (per hour)	6	4.7	-10.9

The thermal gradient associated with greenhouse length in the three configurations can be clearly seen in Figures 9a, 9b and 9c, which represent the average temperature at a height of 2 m as a function of greenhouse length. For the closed-roof greenhouse (Figure 9a), there was a strong linear regression between the increase in temperature and greenhouse length (linear regression equations were shown in Table 4), so that the four simulated greenhouse lengths (28 m, 50 m, 75 m and 100 m) can be represented by a single linear regression, as shown in Figure 9a; with the roof ventilators closed, greenhouse length has to be limited to less than 50 m unless a greenhouse temperature that is 10 K above the outside air temperature is acceptable.

For Configuration 2 (Figure 9b), there was also a good linear regression between temperature and greenhouse length (Table 4), but compared to Configuration 1, the slope of the regression line was lower. For this configuration, greenhouse temperature was also dependent on greenhouse length. Figure 9b shows that the temperature near the inlet wall increased as greenhouse length increased. This can be explained by the fact that natural ventilation makes the greenhouse air exit through the windward area of the roof ventilator (as shown in Figure 5). This air exit creates a backflow in the greenhouse that brings some warm air from the central area to the windward front wall. In spite of the benefits of natural ventilation, as with Configuration 1, it is advisable to limit greenhouse length to avoid excessive temperatures. Otherwise, the fan capacity has to be increased to reduce the change of temperature with length (this will be further discussed below).

Configuration 3 is a different case. Figure 9c shows that for the 100-m-long greenhouse, after the first 50 m, the greenhouse temperature remained nearly constant regardless of greenhouse length. Under the unfavourable conditions of this study (greenhouse under sunny conditions with no transpiring crops), the increase

in temperature was around 10 K for the longest greenhouse.

The air speed inside the greenhouse normalized by the outside wind speed is shown in Figure 10. For the three configurations, the highest speed was found near the inlet wall. The backflow mentioned above was probably responsible for this. The air velocity then became relatively constant, but fluctuated more in Configurations 2 and 3; natural ventilation may interfere with mechanical ventilation by creating this sort of air-speed fluctuation. In any case, with the exception of the first few metres near the inlet wall, the normalized air velocity was within the range of 0.10 to 0.20. The ASABE code of practice for heating and ventilating greenhouses recommends not exceeding an air speed of 1 m/s across the plants; so the air speed in the greenhouses designed using CFD was below the maximum recommended value (for most outside wind speed conditions). It was therefore possible to conduct more simulations with increased fan capacity.

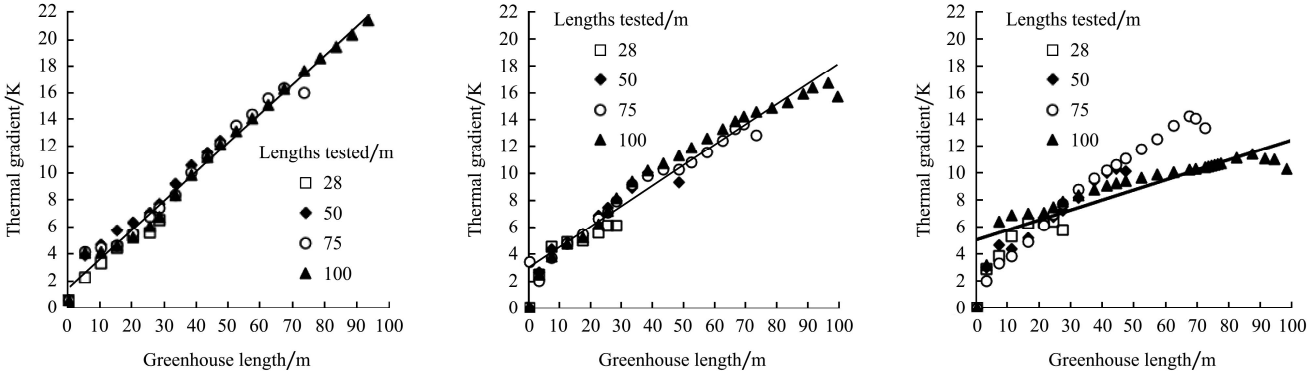

a. Configuration 1 b. Configuration 2 c. Configuration 3

Figure 9 Profile of temperature with greenhouse length for Configurations 1, 2 and 3 at 2 m height. Linear regression adjustments for the 100 m long greenhouse.

Table 4 Linear regressions between inside air temperature difference dT (K) and greenhouse length *x* (m) for three different fan capacities in the 100 m long greenhouse. N1= 10.4 h^{-1}; N2=15.5 h^{-1} and N3=23.7 h^{-1}.

Case studied		Fan capacity (vol h^{-1})		
		N1	N2	N3
Configuration 1	Regression adjustment	$T=0.1967x+2.6647$ $R^2=0.9892$	$T=0.1186x+0.526$ $R^2=0.9945$	$T=0.0752x+0.7274$ $R^2=0.9945$
Configuration 2	Regression adjustment	$T=0.1432x+3.871$ $R^2=0.9706$	$T=0.0995x+4.6342$ $R^2=0.9599$	$T=0.0526x+4.0606$ $R^2=0.8695$
Configuration 3	Regression adjustment	$T=0.0551x+6.4677$ $R^2=0.956$	$T=0.0468x+6.1819$ $R^2=0.9618$	$T=0.0209x+6.0555$ $R^2=0.418$

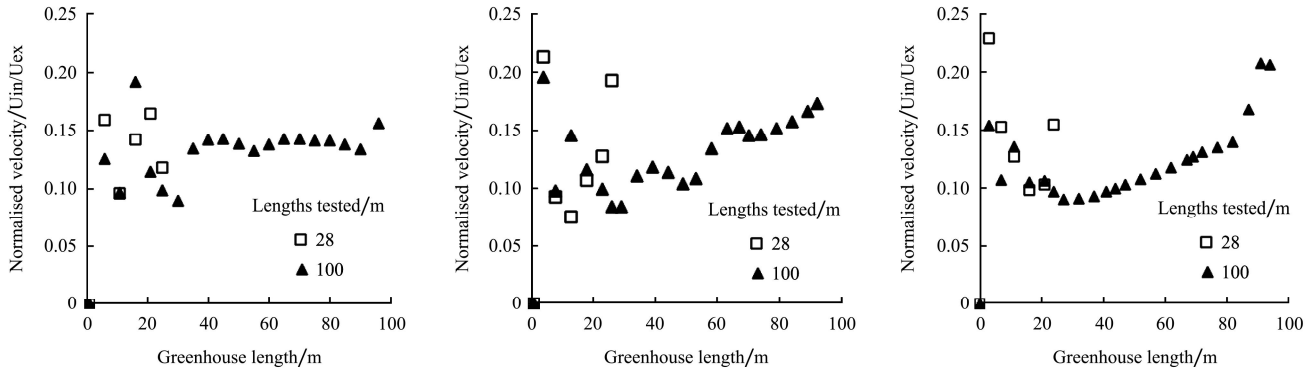

a. Configuration 1 b. Configuration 2 c. Configuration 3

Figure 10 Greenhouse air speed normalized by outside air speed for Configurations 1, 2 and 3 for the 28 m long greenhouse and the 100 m long greenhouse at 2 m height

3.2.2 Effect of fan flow on the temperature regime of mechanically ventilated greenhouses

For the second set of simulations, two different pressure drops across the fans were used to produce air exchange rates of 15.5 and 23.7 air changes per hour in the 100-m-long greenhouse. It was advisable to maintain fan capacity within this range in order to keep the internal air speed within the range recommended by ASABE[4]. For the sake of brevity, simulations were done only for the 100-m-long greenhouses and sections of the appropriate lengths were used to represent the shorter greenhouses.

Figure 11 compares the thermal gradient along the 100-m-long greenhouse for the three configurations and three airflow rates (the one presented in Figure 9 plus the two new ones for this set of simulations). Figure 11a shows the effect of increasing the fan flow for Configuration 1. There is a very good linear regression between temperature and the distance from the inlet wall for the three airflows considered in this study.

Figure 11 showed that for the highest ventilation rate, the increase in temperature had a moderate slope, so that the greenhouse temperature at 100 m from the inlet air wall was approximately 8 K higher than the outside air. This increase in temperature is expected to be lower in greenhouses with a transpiring crop or in greenhouses with an additional cooling method such as evaporative cooling using fog systems[9].

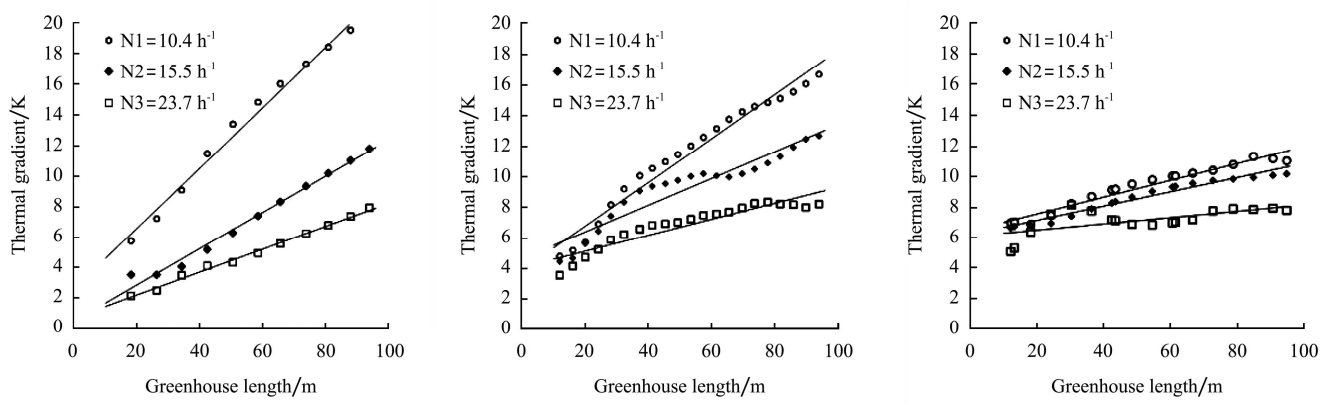

a. Configuration 1 b. Configuration 2 c. Configuration 3

Figure 11 Thermal gradient with greenhouse length and the regression lines for Configurations 1 2 and 3 for three different ventilation rates

3.2.3 Study of the front wall inlet opening

For this third set of simulations, the discrete inlet boxes shown in Figure 1 were replaced by one continuous, rectangular inlet in the front wall measuring 22.5 m long by 1.4 m high (Figure 12). This height was chosen so that it was the same as the height of the inlet box for comparison purposes. With these dimensions, the new inlet area was 3.75 times greater than the area of the fans. The new continuous opening was covered with an insect-proof screen with the same airflow resistance as the one used in the ventilators. The boundary conditions set were the same as the ones used for the study of Configurations 1, 2 and 3. For the sake of brevity, only the results from Configuration 3 with the continuous inlet opening are presented.

Figure 12 shows the map of temperature at a height of 2 m for this greenhouse. This figure can be compared to Figure 8, obtained for the same greenhouse configuration and fan flow, but with a different inlet. The beneficial effect of the increased inlet area can be seen by the temperature reductions in the areas near the inlet wall and the central areas of the greenhouse. The temperature areas near the exhaust fans remained more or less the same as in the greenhouses with the box inlets. At the far end of the greenhouse, the increase in inlet size did not make any significant difference in temperature.

Figure 13 can be considered a summary of this ventilation study. It compares the temperature profile for natural ventilation alone with the best combinations of natural and mechanical ventilation for the configurations studied. Under the demanding conditions imposed for the simulations (high solar radiation, no transpiring crops,

insect-proof netting on the ventilators and wind parallel to the roof ventilators), natural ventilation alone created excessively high greenhouse temperatures with some very hot spots near the windward front wall (Figure 13), given that an internal backflow opposite the external wind direction was created[22].

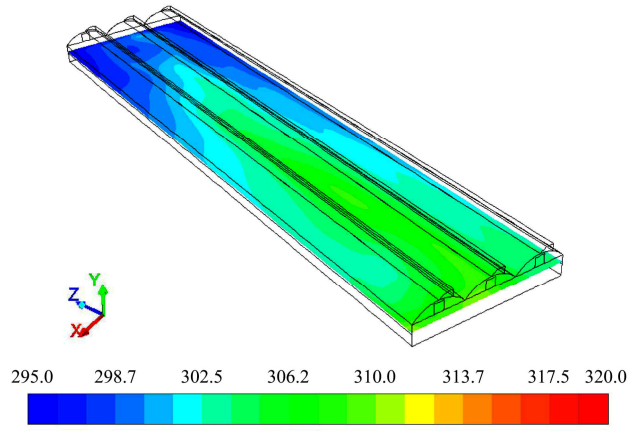

Figure 12 Map of temperature at 2 m height for Configuration 3 with increased inlet area.

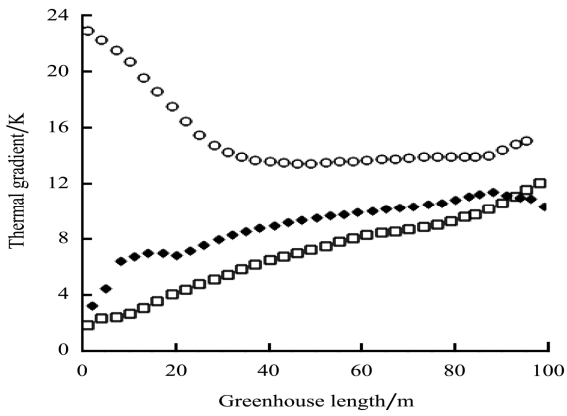

○ With greenhouse length for roof ventilation only (no fan ventilation)
◆ Mechanical ventilation with maximum fan capacity and box inlet
□ Mechanical ventilation with maximum fan capacity and increased inlet area

Figure 13 Comparison of thermal gradient in three cases for Greenhouse with Configuration 3

For the maximum fan capacity tested in this study, the combination of natural and mechanical ventilation created a more favourable temperature regime, and using one enlarged, continuous inlet instead of discrete box inlets further reduced the temperature near the inlet wall because it eliminated the circulation cells observed in Figure 4.

This study highlights the value of using numerical simulations as a way of improving the design of climate control systems for greenhouses. After model validation, simulations can be used to detect the constraints of existing designs, such as the development of undesirable hot spots, and to evaluate design modifications to solve the problems identified. The suggested modifications can be simulated again until a suitable design solution is achieved.

The study showed the merit of combining natural ventilation and mechanical ventilation, although the advantages of this combination depend on greenhouse length. For the 28-m-long experimental greenhouse, the air exchange produced by mechanical ventilation was significantly greater than natural ventilation so the effect of roof ventilators on the internal climate was limited. For longer greenhouses, the relative importance of natural ventilation increased, whereas the air exchange produced by mechanical ventilation remained nearly the same. As a consequence, the combination of the two ventilation methods is more advantageous for long greenhouses.

It is important to note that the air exchange rate is not necessarily a good indicator of the efficiency of the ventilation system. As mentioned by some studies[17,18], a high ventilation rate does not guarantee the uniformity of the greenhouse climate. Natural ventilation combined with mechanical ventilation produced better mixing of the internal air. As a result, the temperature distribution for Configurations 2 and 3 was more uniform than for mechanical ventilation alone, as shown by the slope of the regression lines for the greenhouses.

The results for Configuration 3 were more favourable than those for Configuration 2. If the greenhouse has roof ventilators, it seems reasonable to open them as much as possible. The partial opening of the roof ventilators was tested to address the concern of having an inconvenient flow pattern due to the combination of fan and roof ventilation, but this situation did not arise.

This study shows that for 100-m-long greenhouses it is possible to keep the interior temperature to less than 7 K above the outside air under unfavourable conditions (no transpiring crop, high solar radiation, low external wind speed and insect-proof screens on the ventilators). To achieve this goal, mechanical ventilation has to be combined with natural ventilation. Also, the fans should be able to provide air exchange values close to 25 vol/h

and the air inlet area should be significantly larger than the area of the fans (3.75 times larger for this study).

The results presented in this study should help in the design of more efficient mechanical ventilation systems. Nevertheless, some related subjects must be addressed; in particular the response of the greenhouse to winds not parallel to the greenhouse axis and the effect of combined ventilation for structures with widths of more than three spans.

4 Conclusions

A 3D numerical simulation model of a fan-ventilated and roof-ventilated greenhouse was developed and validated by experimentation. For the three configurations studied (mechanical ventilation alone, mechanical ventilation plus roof ventilators open 30% and mechanical ventilation plus roof ventilation open 100%), the agreement between experimental and simulated values was good in terms of the air exchange rate and temperature distribution.

Roof ventilation combined with mechanical ventilation improved the air exchange rate and climate uniformity of the greenhouse due to better mixing of the internal air than the mixing produced with mechanical ventilation alone. The effect of roof ventilation was more relevant for 100-m-long greenhouses than for the shorter experimental greenhouse.

In most of the cases studied, there was a strong linear correlation between the temperature gradient and greenhouse length. The regression line with the steepest slope was the one for the greenhouse with closed roof ventilators.

As expected, increasing the fan capacity produced a general reduction in temperature, but the effect was less pronounced for the roof-ventilated greenhouses. Maximum fan capacity is limited by the maximum tolerable air speed in the canopy area to avoid plant damage.

Compared to the box inlet ventilators, an enlarged, continuous inlet in the wall opposite the fans increased overall system performance because it eliminated backflow recirculation zones, which are prone to produce high temperatures.

Under the unfavourable conditions considered in this study, it is possible to have good ventilation in 100-m-long greenhouses, provided that the recommendations suggested in this analysis are taken into consideration.

Acknowledgements

This research work was partially financed by the EUPHOROS project, Efficient Use of inputs in Protected Horticulture, the Seventh EU Framework Programme and INIA project RTA (2008-00109-C03-01). Many thanks are given to Dr. Bernard J. Bailey for his assistance reviewing the manuscript and to Dr. Santiago Bonachela for his valuable comments. CONACYT-Mexico provided financial support for Dr. Jorge Flores-Velazquez during his stay in Spain.

Notations

$c(t)$	Tracer gas concentration in time t, ppm
c_o	Initial tracer gas concentration, ppm
p	Air pressure, Pa
t	Time, s
u	Air velocity, m/s
H_{sc}	Heat transferred from soil surface to greenhouse air, W/m^2
Q_{soil}	Soil heat flux to deep ground, W/m^2
RI	Outside solar radiation, W/m^2
RI_a	Fraction of radiation that passes through the film cover, W/m^2
R_α	Radiation fraction reflected
V_t	Air exchange rate, per hour
Φ	Concentration of transported quantity
Γ	Diffusion coefficient, m^2/s
S_Φ	Source term
α	Albedo
ε	Screen porosity
∂p	Drop in pressure through a porous media, Pa
∂x	Thickness of the porous media, m
γ	Overall greenhouse transmissivity
ρ	Density of air, kg/m^3
μ	Kinematic viscosity of air, m^2/s
K	Permeability of the medium, m^2
C_F	Non-linear momentum loss coefficient

[References]

[1] Mistrotis A, Bot G P A, Picuno P, Scarascia-Mugnozza G. Analysis of the efficiency of greenhouse ventilation using computational fluid dynamics. Agricultural and Forest Meteorology, 1997; 85: 217-228.

[2] Kittas C, Karamanci M, Katsoulas N. Air temperature in a forced ventilation greenhouse with rose crop. Energy and buildings, 2005; 37: 807-812.

[3] Bailey B J, Montero J I, Perez-Parra J, Robertson A P, Baeza E, Kamaruddin R. Airflow resistance of greenhouse ventilators with and without insect screens. Biosystems Engineering, 2003; 86: 217-229.

[4] ASABE. Heating, ventilating and cooling greenhouses, ANSI/ASAE Standard EP406.4. 2003, 699-707.

[5] Willits D H, Li S, Yunker C A. The cooling performance of naturally ventilated greenhouse in the Southeastern US. Acta Horticulturae (ISHS), 2006; 719: 73-82.

[6] Fidaros D, Baxevanou C, Bartzanas T, Kittas C. Flow Characteristics and temperature patterns in a fan ventilated greenhouse. Acta Horticulturae (ISHS), 2008; 797: 123-130.

[7] Montero J I, Short T, Curry R B, Bauerle W L. Influence of evaporative cooling systems on greenhouse environment. ASAE paper: 81-4027, 1981; pp 15.

[8] Al-Helal I M. Effect of ventilation rate on the environment of a fan-pad evaporatively cooled, shaded greenhouse in extreme arid climates. Applied Engineering in Agriculture, 2007; 23(2): 221-230.

[9] Arbel A, Yekueteli O, Barak M. Performance of a fog system for cooling greenhouses. Journal of Agricultural Engingeering Research, 1999; 72(2): 129-136.

[10] Kittas C, Katsoulas N, Baille A. Influence of greenhouse ventilation regime on microclimate and energy partionating of a rose canopy during summer conditions. Journal of Agricultural Engineering Research, 2001; 79(3): 349-360.

[11] Kittas C, Bartzanas T, Jaffrin A. Temperature gradients in a partially shaded large greenhouse equipped with evaporative cooling pads. Biosystems Engineering, 2003; 85(1): 87-94.

[12] Arbel A, Barak M, Shklyar A. Combination of forced ventilation and fogging systems for cooling greenhouses. Biosystems Engineering, 2003; 84(1): 45-55.

[13] Baeza E J, Bailey B J, Pérez-Parra J, Gazquez J C, López J C. Perfiles de temperatura y circulación de aire en un invernadero multitúnel con ventilación forzada. 3º Congreso Nacional de Agroingenieria, León, España, 2005; 21-24.

[14] Campen J B, Bot G P A. Determination of greenhouse aspects of ventilation using three-dimensional computational fluid dynamics. Biosystems Engineering, 2003; 84(1): 69-77.

[15] Kacira M, Sase S, Okushima L. Optimisation of vent configuration by evaluating greenhouse and plant canopy ventilation rates under wind-induced ventilation. Transaction of the ASABE, 2004; 47(6): 2059-2067.

[16] Baeza E J, Pérez-Parra J J, Montero J I. Effect of ventilator size in natural ventilation of parral greenhouse by means of CFD simulations. Acta Horticulturae (ISHS), 2005; 691: 465-472.

[17] Bartzanas T, Boulard T, Kittas C. Effect of vent arrangement on windward ventilation of a tunnel greenhouse. Biosystems Engineering, 2004; 88(4): 479-490.

[18] Ould Khaoua S A, Bournet P E, Migeon C, Boulard T, Chasseriaux G. Analysis of greenhouse ventilation efficiency based on computational fluid dynamics. Biosystems Engineering, 2006; 95: 83-98.

[19] Norton T, Sun D, Grant J, Fallon R, Dodd V. Application of computational fluid dynamics (CFD) in the modeling and design of ventilation systems in the agricultural industry: A review. Bioresource Technology, 2007; 98(12): 2386-2414.

[20] Baeza J E. Optimización del diseño de los sistemas de ventilación en invernadero tipo parral. PhD Dissertation, 2007; Universidad de Almería, Almería, Spain.

[21] Boulard T, Meneses J F, Mermier M, Papadakis G. The mechanism involved in the natural ventilation of greenhouse. Agricultural and Forrest Meteorology, 1996; 79: 61-77.

[22] Boulard T, Draoui B. Natural ventilation of a greenhouse with continuous roof vents: measurement and data analysis. Journal of agricultural Engineering Research, 1995; 61: 27-36.

[23] Roy J C, Boulard T, Kittas C, Wang S. Convective and ventilation transfer in greenhouses: Part 1: The greenhouse considered as a perfectly stirred tank. Biosystems Engineering, 2002; 83(1): 1-20.

[24] Patankar S V. Numerical heat transfer and fluid flow. (1st ed.). Washington: McGraw-Hill, 1980; DOI: 10.1615/ AtoZ.n.numerical_heat_transfer

[25] Anderson J D. Computational fluid dynamics. The basics with applications. (1st ed.). Columbus: McGraw-Hill, 1995; (Chapter 1).

[26] Miguel A F, Van de Brank N J, Bot G P A. Analysis of the airflow characteristics of greenhouse screening materials. Journal of Agricultural Engingeering Research, 1997; 67: 105-112.

[27] Valera D L, Álvarez A J, Molina F D. Aerodynamic analysis of several insect-proof screens used in greenhouses. Spanish Journal of Agricultural Research, 2006; 4(4): 273-279.

[28] Teitel M. The effect of insect-proof screens in roof openings on greenhouse microclimate. Agricultural and Forest Meteorology, 2001; 110: 13-25.

[29] Kamaruddin R. A naturally ventilated crop protection

structure for tropical conditions. PhD Dissertation, 1999; University of Cranfield, Cranfield, United Kingdom.

[30] Cabrera F J, Lopez J C, Baeza E J, Pérez-Parra J. Efficiency of anti-insect screens placed in the vents of Almeria greenhouses. Acta Horticulturae (ISHS), 2006; 719: 605-614.

[31] Flores-Velazquez J, Montero J I. Computational Fluid Dynamics (CFD) study of large scale screenhouses. Acta Horticulturae (ISHS), 2008; 797: 117-122.

[32] Teitel M. Using computational fluid dynamics simulations to determine pressure drops on woven screens. Biosystem Engineering, 2010; 105: 172-179.

[33] ANSYS Inc. Pittsburgh PA USA. ANSYS CFX Release 12.1 User Guide, 2009.

[34] Launder B E, Spalding D B. Lectures in mathematical models of turbulence. (1st ed.). London: Academic Press, 1972 (Chapter 2). pp 169.

[35] Lee I B, short T H. Verification of computational fluid dynamic temperature simulations in a full-scale naturally ventilated greenhouse. Transactions of the ASAE, 2001; 44(1): 119-127.

[36] Bartzanas T, Kittas C, Sapounas A A, Nikita- Martzopoulou C. Analysis of airflow through experimental rural buildings: Sensitivity to turbulence models. Biosystems Engineering, 2007; 97(2): 229-239.

[37] Flores-Velazquez. Análisis del clima en los principales modelos de invernaderos en México (malla sombre, multitúnel y baticenital) mediante la técnica CFD (Computational Fluid Dynamics). PhD Dissertation, 2010; Universidad de Almeria, Almeria, Spain.

[38] Stull R B. Meteorology for scientist & engineers (2nd ed.). Brooks/cole Thompson learning. 2000; pp 502.

[39] Ducarme D, Vandaele L, Wouters P. Single sided ventilation: a comparison of the measured air change rates with tracer gas and with the heat balance approach. Documentation for BAG Meeting on Ventilation Related Aspects in Buildings, 1994; pp 26-35.